Theor Chem Account (2008) 119:133–142
DOI 10.1007/s00214-006-0186-1

REGULAR ARTICLE

Direct determination of absolute configuration: a vibrational circular dichroism study on dimethyl-substituted phenyloxiranes synthesized by Shi epoxidation

Peter Fristrup · Peter Rygaard Lassen · David Tanner · K. J. Jalkanen

Received: 1 June 2006 / Accepted: 13 November 2006 / Published online: 19 December 2006
© Springer-Verlag 2006

Abstract The three possible dimethylsubstituted phenyloxiranes (*cis, trans* and *geminal*) were synthesized in both racemic (*m*CPBA) and enantiomerically enriched forms (Shi epoxidation) and subjected to a vibrational circular dichroism study. The experimental spectra were compared to theoretical spectra obtained using DFT/B3LYP calculations, and the differences between experiment and theory are discussed. The absolute configuration at the benzylic position was established as being (*R*), (*S*) and (*R*) for the *cis, trans* and *geminal* dimethylsubstituted phenyloxiranes, respectively. In all three cases the configuration of the major enantiomer was in accordance with a simple transition state model based on the *spiro* reaction mode.

Keywords Vibrational circular dichroism · DFT calculations · Epoxidation · Asymmetric catalysis · Absolute configuration

Electronic supplementary material The online version of this article (http://dx.doi.org/10.1007/s00214-006-0186-1) contains supplementary material, which is available to authorized users.

P. Fristrup (✉)
Center for Sustainable and Green Chemistry, Department of Chemistry, Technical University of Denmark, Building 201, Kemitorvet, Lyngby 2800, Denmark
e-mail: pf@kemi.dtu.dk

P. Fristrup · D. Tanner
Department of Chemistry, Technical University of Denmark, Building 201, Kemitorvet, Lyngby 2800, Denmark

P. R. Lassen · K. J. Jalkanen
The Quantum Protein Centre, Department of Physics, Technical University of Denmark, Building 309, Lyngby 2800, Denmark

K. J. Jalkanen
Nanochemistry Research Institute, Department of Applied Chemistry, Curtin University of Technology, GPO Box U1987, Perth, WA 6845, Australia

1 Introduction

Chiral, non-racemic oxiranes (epoxides) are very useful intermediates in organic synthesis, [1–5] and the past two decades have seen remarkable progress in the development of methods for the enantioselective epoxidation of alkenes. [6] Apart from the metal-catalyzed processes pioneered by Sharpless [7,8], Jacobsen [9,10] and Katsuki [11,12], one of the most interesting developments in the field is the Shi methodology [13–16] based on the *in-situ* formation of chiral dioxiranes from readily available chiral ketones (Fig. 1).

Mechanistically, the enantioselectivity in the reaction has been proposed to arise from a differentiation between several possible transition states of both *spiro* and *planar* geometry (Fig. 2) [16]. However, the major enantiomer is always believed to originate from a *spiro* transition state and its formation can be predicted by careful consideration of steric interactions between the alkene and the catalyst. Experimental fine-tuning of steric [17,18] and electronic [19,20] features based on this selectivity model has led to new catalysts specifically designed for alkene subclasses, such as *cis*-disubstituted alkenes [21] and terminal alkenes [22]. Recently, these rationalizations of experimental findings have been further substantiated by the experimental determination of kinetic isotope effects for the epoxidation of *trans*-β-methylstyrene, which were in good agreement with quantum mechanical calculations [23].

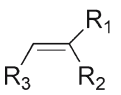

Fig. 1 General scheme for the Shi epoxidation using a chiral ketone derived from D-fructose

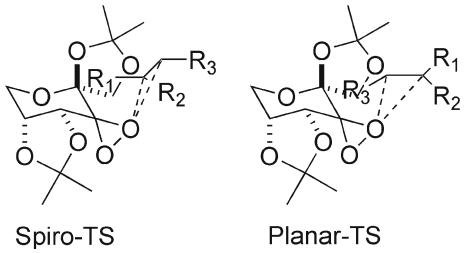

Fig. 2 The selectivity model developed by Shi and coworkers for prediction of absolute configuration [14]. In all cases the major enantiomer arises from a *spiro*-type TS (*left*), whereas the minor enantiomer is produced via a *planar*-TS (*right*)

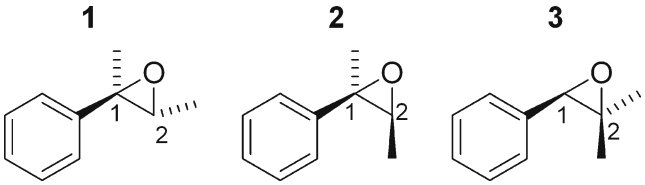

Fig. 3 The compounds investigated here are (*1R*, *2R*)-1, 2-dimethylphenyloxirane (**1**), (*1R*, *2S*)-1, 2-dimethylphenyloxirane (**2**) and (*1R*)-2, 2-dimethylphenyloxirane (**3**). For all three compounds the enantiomer having the (*R*)-configuration at the benzylic position has been drawn for simplicity

We became particularly interested in the Shi epoxidation in connection with a general project aimed towards the development and refinement of methods for the direct determination of the absolute configuration of small organic molecules [24]. In this paper we present a study of the three dimethyl-substituted phenyloxiranes (**1–3**) which were obtained in enantiomerically enriched form via Shi epoxidation; we have combined experiment (vibrational circular dichroism, VCD) and theory (DFT/B3LYP calculations) in order to directly assign the absolute configuration of these chiral epoxides (Fig. 3).

2 Results and discussion

2.1 Conformational search

Both the oxirane ring and the phenyl ring are very rigid molecular entities with no internal degrees of freedom. Each of the methyl groups has a threefold symmetry

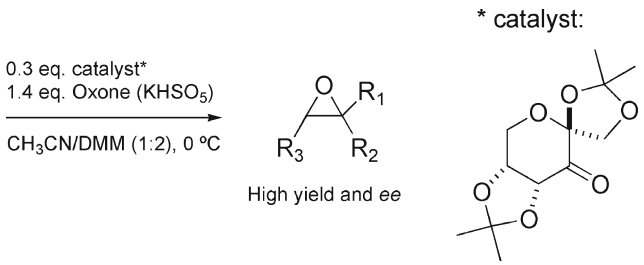

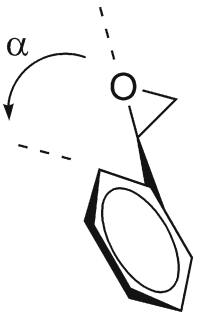

Fig. 4 Definition of the dihedral angle which was used to calculate the energy barrier for rotation of the phenyl group

axis; however, they will relax during an energy minimization and not give rise to multiple conformers. This narrows down the conformational search to the rotation of the phenyl ring with respect to the plane of the oxirane ring. The question of existence of different conformers, each having a different value of the dihedral angle, α (as illustrated in Fig. 4) has been addressed by calculation of the total energy of the molecules at different fixed dihedral angles to generate the torsional (dihedral) angle potential energy surface.

The energy profiles are plotted in Fig. 5 with respect to the energy minimum for the most stable conformation of **3**.

For all three phenyloxiranes **1–3** only one favored conformation exists (Fig. 5), albeit with small differences in the preferred orientation of the phenyl group. The primary stabilizing interaction is a hydrogen bond between the oxygen atom and the proximal hydrogen on the phenyl ring. The presence of only one low-energy conformation allowed us to limit the lengthy calculation of spectroscopic properties to one minimum energy conformation for each molecule.

2.2 Vibrational absorption (VA)

The calculated absorption spectrum and experimental spectrum (neat liquid) for **1–3** are shown in Figs. 6, 7 and 8. Structurally, all three compounds are very similar, which result in quite similar VA spectra. For instance, the chosen wavenumber range (900–1,600 cm^{-1}) corresponds to fundamentals no. 22–49 for all three compounds out of a total of 63 fundamentals for a molecule with 23 atoms (3N-6). In general, the agreement between experiment and theory is excellent, allowing for a direct assignment of most of the experimental

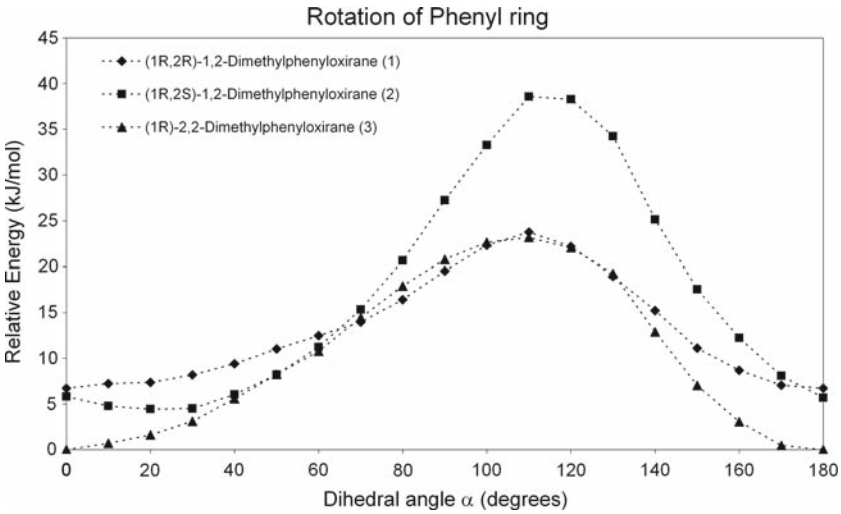

Fig. 5 Relative energies for rotation of the phenyl ring in compounds **1–3**. All energies are relative to the minimum energy conformation of **3**

absorptions to fundamentals determined theoretically. A visualization of the fundamentals 22–49 for all three compounds has been included as supporting information [25]. Initially, all of the experimental absorptions appear at lower wavenumber than the calculated ones, which is mainly due to anharmonicity not accounted for in the calculation, and to remedy this we have chosen to scale the calculated frequencies by 0.98. The predicted intensities (molar extinction coefficient, ε) are in excellent agreement with the experimental measurements. VA spectra were also obtained in CCl_4 but have been omitted as they were virtually identical to the spectra obtained on the neat liquids.

Starting from the low wavenumber side with the VA spectra of **1** (Fig. 6), fundamental 23 is the first absorption fully included in the experimental spectrum.

Compared to the neighboring fundamental 25, the intensity in the calculation may be slightly underestimated. Fundamentals 25 and 28 show very good agreement between theory and experiment. Fundamentals 30 and 31 are separated by only $5\,cm^{-1}$ in the theoretical calculation, but appear as a single absorption in the experimental spectrum. Fundamental 32 seems to have been underestimated in the calculation. There is a good agreement between experiment and theory for fundamentals 33, 35 and 36, whereas for fundamentals 37, 38 and 39 there are differences. The relative intensity of fundamental 37 is overestimated in the calculation, and the relative position is slightly inaccurate. In the experimental spectrum, modes 37, 38 and 39 are evenly spaced with respect to the scale (wavenumbers), whereas in the calculation only 38 and 39 appear together with fundamental 37 appearing isolated at significantly lower wavenumbers. The dipole strengths of fundamentals 42 and 49 are underestimated in the calculation and since the fundamentals 43–48 appear as a single broad absorption in the experimental spectrum the agreement is difficult to comment upon.

When examining the VA spectra of **2** (Fig. 7) the relative intensity of fundamental 22 compared to 23 is overestimated in the calculation.

Furthermore for fundamental 29 compared to 28 there exists a disagreement between experiment and theory for the relative intensities, and even more for fundamental 30 when compared to 31. In spite of this, the pattern consisting of fundamentals 28–34 is easily recognized and interpreted. This is also the case for fundamentals 37, 39 and the combined absorption profile for fundamentals 41 and 42. Also fundamental 49 appears to be well separated at the high wavenumber end of the spectrum and is in good agreement with the experimental spectrum. Fundamental 43 seems to be overestimated in the calculation (compared to fundamentals 41 and 42) and the combined absorption profile for fundamentals 44–47 gives rise to a strong, sharp absorption in the experimental spectrum in contrast with a very broad calculated absorption profile.

The calculated and experimental VA spectra for **3** are shown in Fig. 8. For this compound fundamentals 22 and 23 appear as a single absorption in both the calculated and the experimental spectrum.

When comparing the absorptions arising from fundamentals 29 and 30 they are closer together in the experimental spectrum than the predicted spectrum. In contrast, fundamentals 31 and 32 are more separated in the experimental spectrum than in the calculated spectrum. Fundamentals 33 and 37 give rise to very strong absorptions and are easily recognizable. In the experimental spectrum fundamentals 38, 39 and 40 are nicely separated while in the calculated spectrum fundamentals 39 and 40 are very close together ($7\,cm^{-1}$). As for the two other compounds, the fundamentals 41

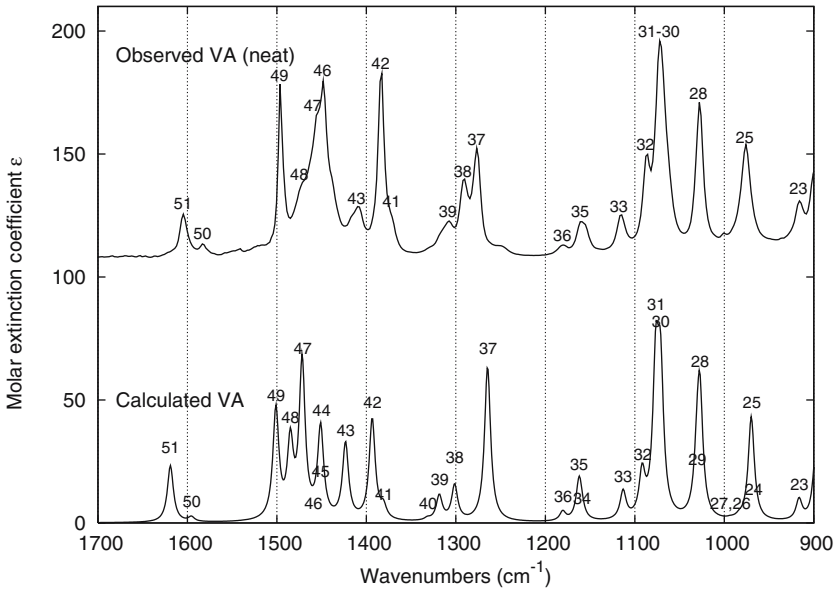

Fig. 6 Comparison of calculated VA spectrum (6-31++G** basis set, *bottom*) with experimental spectrum obtained for (*1R*, *2R*)-1, 2-dimethylphenyloxirane (**1**) as a neat liquid (*top*)

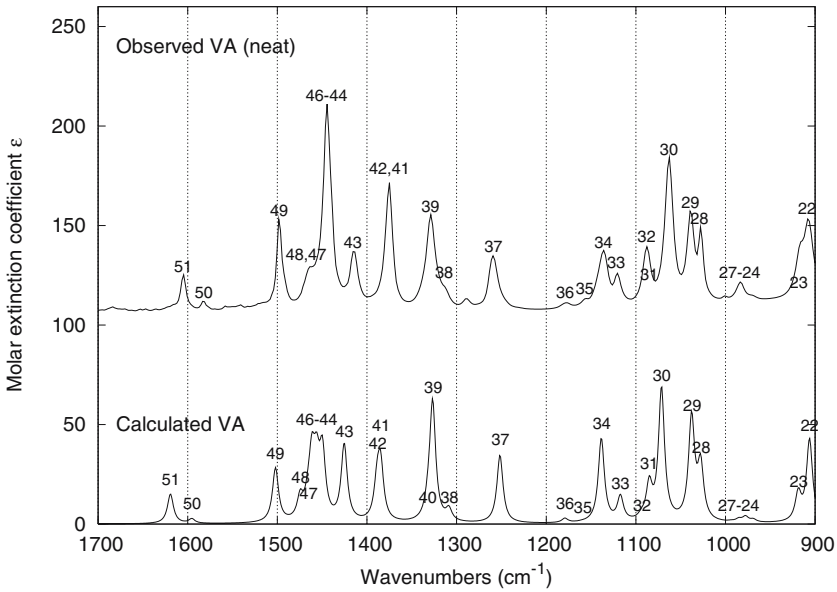

Fig. 7 Comparison of calculated VA spectrum (6-31++G** basis set, *bottom*) with experimental spectrum obtained for (*1S*, *2R*)-1, 2-dimethylphenyloxirane (**2**) as a neat liquid (*top*)

and 42 give rise to only one, broad absorption band in the experimental spectrum, whereas fundamental 43 is fully resolved. This is not the case for fundamentals 45–47 which appear as a broad, almost triangular-shaped absorption in the experimental spectrum. As for the two other compounds, fundamental 49 is fully separated at the high wavenumber end of the spectrum.

2.3 Vibrational circular dichroism (VCD)

The calculated and experimental vibrational circular dichroism spectra for **1–3** are shown in Figs. 9, 10 and 11. The experimental spectra were obtained both for the neat liquid and the CCl_4 solution and in contrast to the results obtained for VA there are now distinct differences. Compared to the VA spectra the signal-to-noise ratio is significantly lower, resulting in only the strongest absorptions giving reliable information. In contrast to the VA spectra, where there was excellent agreement between the calculated and observed molar absorptivity (ε), the predicted VCD intensities are now frequently a factor of 2–4 smaller. This could arise from the fact that we have used the 6-31++G** basis and not the larger aug-cc-pVDZ or aug-cc-pVTZ basis sets, which have been shown to give slightly better correlation to experiment for phenyloxirane [26,27]. However, in this study we are mainly concerned with the prediction of absolute configurations, for which the 6-31++G** basis set is deemed sufficient.

The calculated and experimental VCD spectra for **1** are shown in Fig. 9. Again, starting from the lower wavenumbers, fundamentals 28 and 29 are the first

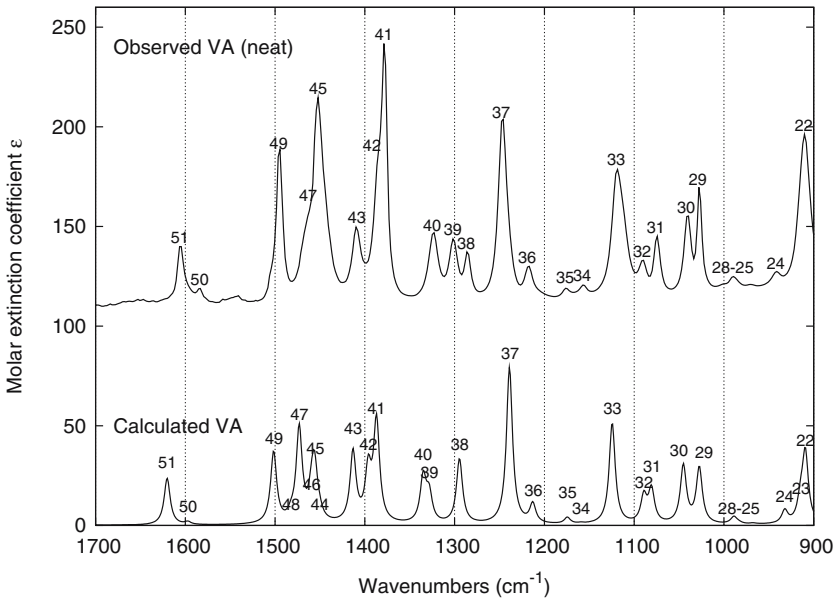

Fig. 8 Comparison of calculated VA spectrum (6-31++G** basis set, *bottom*) with experimental spectrum obtained for (*1R*)-2, 2-dimethylphenyloxirane (**3**) as a neat liquid (*top*)

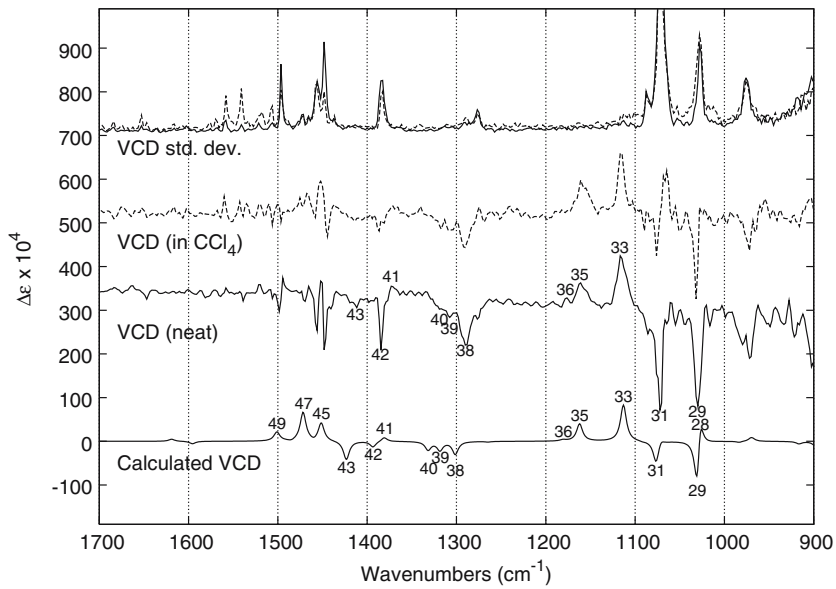

Fig. 9 Comparison of calculated VCD spectrum (6-31++G** basis set, *bottom*) with experimental spectra obtained for (*1R*, *2R*)-1, 2-dimethylphenyloxirane (**1**) as a neat liquid and in CCl_4 solution

absorptions calculated to have medium to strong intensity. The separation is only $3\,cm^{-1}$ (as calculated) for the two bands which are of different sign, resulting in an extinction of the positive VCD in the experimental spectra, while the overall negative VCD signal is well reproduced, both for the neat liquid and for the CCl_4 solution. The positive VCD arising from the combination of fundamentals 32 and 33 is in good agreement with the experimental spectra which is also the case for fundamental 35. Interestingly, the weak negative VCD from fundamentals 38, 39 and 40 results in one medium-intensity VCD absorption in the experiment along with some minor neighboring absorptions. Measurements at higher wavenumber are hampered by the accompanying high absorbance, thus yielding a relatively high uncertainty for the VCD signal.

In conclusion, the synthesized 1,2-dimethylphenyloxirane **1** could be assigned as being the (*1R*, *2R*)-enantiomer based on correlation between experimental and calculated VCD for bands 29, 31, (32/33), 35, 38 and 42.

The calculated and experimental VCD spectra for **2** are shown in Fig. 10. The calculated VCD spectrum has been multiplied by −1 to allow for easier comparison to the experimental spectra once the sign of the VCD spectra made it apparent that we have simulated the spectrum for the other enantiomer. Fundamental 25 is predicted to have a positive VCD which is also observed experimentally, although the region is quite noisy. Fundamental 29 is predicted to have a strong negative VCD which is seen in the experimental spectra. An additional absorption is observed in the experimental spectra from fundamental 28, for which the intensity

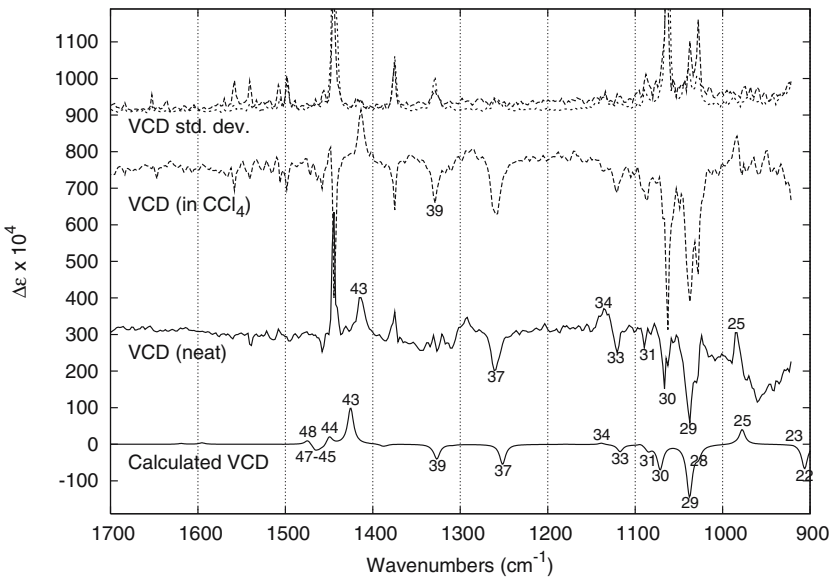

Fig. 10 Comparison of calculated VCD spectrum (6-31++G** basis set, *bottom*) with experimental spectra obtained for (*1S*, *2R*)-1, 2-dimethylphenyloxirane (**2**) as a neat liquid and in CCl_4 solution

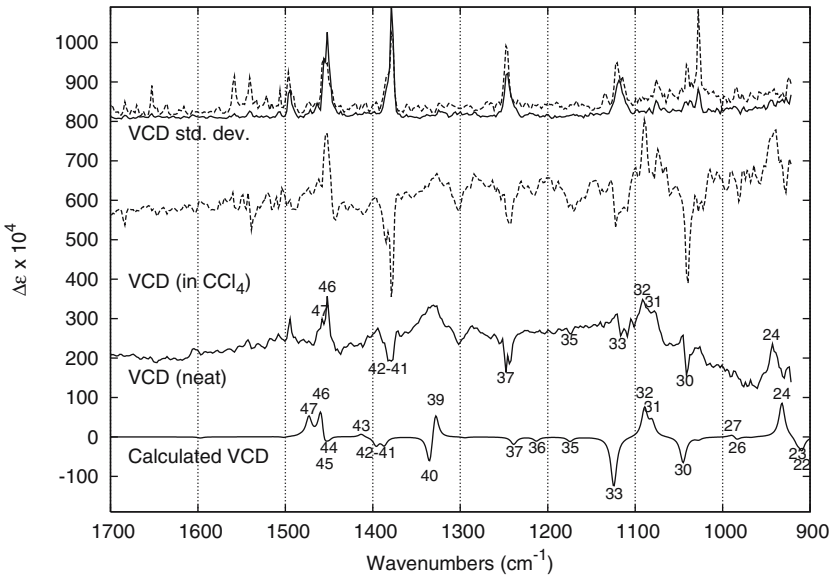

Fig. 11 Comparison of calculated VCD spectrum (6-31++G** basis set, *bottom*) with experimental spectra obtained for (*1R*)-2, 2-dimethylphenyloxirane (**3**) as a neat liquid and in CCl_4 solution

is underestimated in the calculation. The three negative absorptions from fundamentals 30, 31 and 32 are in good agreement with the experimental spectra although the relative intensity of fundamental 30 is overestimated in the calculation. For the absorption arising from fundamental 37 there is a good agreement between the calculated and experimental bands. The weaker fundamental 39 is seen only in CCl_4 solution and not in the spectra for the neat liquid. Also for fundamental 43 there is a good agreement between theory and experiment, although the relative intensity of this absorption is overestimated in the calculation. The remaining minor absorptions 44–48 were not seen in the experimental spectra, probably due to relatively high noise level in this region. Unfortunately, both experimental spectra contain an artifact at ca. 1,460 cm^{-1}, which is probably related to the very high absorbance in this region. In conclusion the synthesized 1,2-dimethylphenyloxirane **2** could be assigned as being the (*1S, 2R*)-enantiomer based on correlation between experimental and calculated VCD for the fundamentals 25, 28, 29, 30, 31, 33, 37, 39 and 43.

In Fig. 11 the calculated and experimental VCD spectra for **3** are shown. The low wavenumber end of the spectra obtained for the neat liquid has a high noise level, which complicates the comparison to the calculated intensities although the positive signal from fundamental 24 seems reliable as this is also seen in

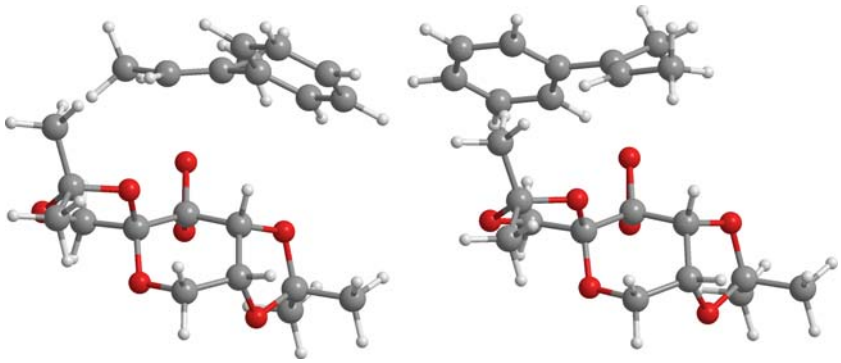

Fig. 12 *Left* The *spiro*-TS for epoxidation of (*E*)-1, 2-dimethylstyrene, which leads to formation of (*1R*, *2R*)-1, 2-dimethylphenyloxirane (**1**). *Right* The competing *planar*-TS for epoxidation, which leads to the minor (*1S*, *2S*)-enantiomer of **1**

CCl_4 solution. Fundamental 30 gives a negative signal of medium intensity which is in good agreement with the experimental spectrum in CCl_4. The positive signal from fundamentals 31 and 32 followed by a negative signal from fundamental 33 is not very clear in the spectrum of the neat liquid, but markedly better in the spectrum obtained for the CCl_4 solution. The predicted strong negative signal from fundamental 33 is not seen clearly in the experiments, which may indicate an overestimation in the calculation. Fundamentals 35, 36 and 37 are predicted to have low intensity and are accordingly difficult to pin-point in the experimental spectra. The positive signal from fundamental 39 is probably more or less cancelled by the negative signal from fundamental 40. Interestingly, the weak absorptions from fundamentals 41 and 42 give rise to medium intensity absorptions in the experimental spectra. The positive absorptions from fundamentals 46 and 47 are in good accordance with the experimental spectra. In conclusion the synthesized 2,2-dimethylphenyloxirane **3** could be assigned as being the (*1R*)-enantiomer based on correlation between experimental and calculated VCD for the fundamentals 24, 30, 31, 32, 33, 37, 41, 42, 46 and 47.

2.4 Molecular modeling

For the tri-substituted alkenes used here there exist two approach vectors which bring the double bond in proximity of the accessible equatorial oxygen atom in the dioxirane. These two approach vectors lead to the well-known *spiro*- and *planar*-type TS discussed earlier, and taking into account the importance of asynchronicity as documented by Singleton and Wang for *trans*-β-methylstyrene the degree of chiral induction (**1** > **2** > **3**) can be explained as follows: the presence of a phenyl group as R_1 favors the *spiro*-TS, where the longer $O-C_\alpha$ distance acts to relieve steric interactions between the phenyl group and the proximal axial hydrogen atom in the catalyst. In the *planar* TS, which is presumed to lead to the formation of the minor enantiomer, the methyl group interacts with the axial hydrogen atom, an interaction which is pronounced by the inherent asynchronicity of the reaction. Furthermore, the relatively large phenyl group could encounter a steric repulsion from the methyl group in the *spiro*-dioxolane moiety. In Fig. 12 structures from a molecular modeling of the two competing TS for epoxidation of **1** are shown [28].

For **2** the *spiro*-TS is favored (cf. **1**) the only difference being that a methyl group is now proximal to the axial hydrogen atom. The *planar*-TS is still disfavored due to the shorter C_β–O bond, but there is no additional penalty since the phenyl group is now pointing away from the catalyst and there is no interaction between the substrate and the *spiro*-dioxolane moiety (Fig. 13). This difference can explain the lower selectivity when comparing **2** to **1**, although a more rigorous computational approach must be taken to verify this.

For the *spiro* TS leading to the formation of **3** (Fig. 14) the asynchronicity of the reaction enhances the steric clash between the methyl group in the substrate and the axial hydrogen atom in the catalyst. Simultaneously, in the *planar* TS leading to formation of the minor enantiomer the unfavorable interactions between the phenyl group and the axial hydrogen atom are relieved. These two factors taken together nicely rationalize the significantly lower selectivity in the asymmetric epoxidation of 2,2-dimethylstyrene compared to the two other dimethyl-substituted styrenes in this study.

3 Conclusion

Three dimethylsubstituted phenyloxiranes were synthesized and their absolute configuration established by comparison of theoretical and experimental VCD spectra. For compounds **1** and **3** the synthesized enantiomer had the (*R*)-configuration at the benzylic position, which confirms assumptions in the literature based on

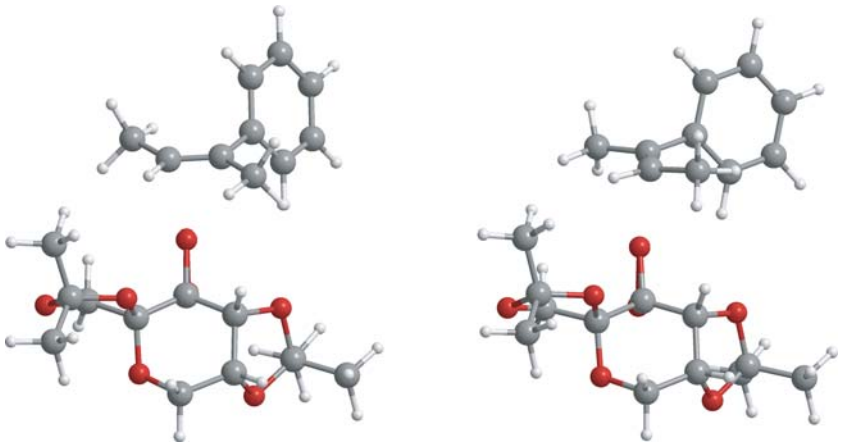

Fig. 13 *Left* The *spiro*-TS for epoxidation of (*Z*)-1, 2-dimethylstyrene, which leads to formation of (*1S*, *2R*)-1, 2-dimethylphenyloxirane (**2**). *Right* The competing *planar*-TS for epoxidation, which leads to the minor (*1R*, *2S*)-enantiomer of **2**

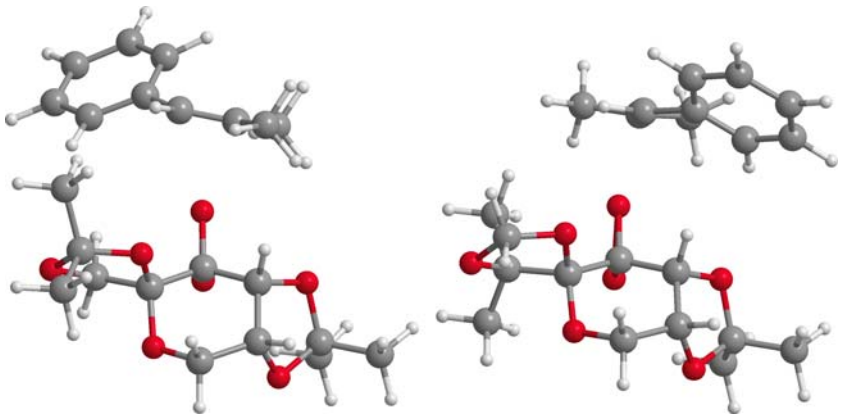

Fig. 14 *Left* The *spiro*-TS for epoxidation of 2, 2-dimethylstyrene, which leads to formation of (*1R*)-2, 2-dimethylphenyloxirane (**3**). *Right* The competing *planar*-TS for epoxidation, which leads to the minor (*1S*)-enantiomer of **3**

the *spiro* reaction mode [15]. The earlier study used a *Z*/*E*-mixture of 2-phenyl-2-butene (1:5), where **2** was isolated as the minor component with an *ee* of 83% without determination of the absolute configuration. In this study we have shown that **2** has the (*S*)-configuration at the benzylic position when synthesized using the Shi epoxidation. This is in contrast to most other substrates in this reaction [14], but in good agreement with the selectivity model developed by Shi and coworkers and has been further substantiated by a molecular modeling study. The three dimethyl-substituted phenyloxiranes used here provide an excellent testing ground for theoretical predictions of reactivity and selectivity. This study also shows how the experimental technique of VCD spectroscopy along with rigorous DFT calculations using a large basis set can give direct access to absolute configuration.

4 Experimental section

Conformational energies were calculated with Jaguar 4.7 [29] using DFT with the B3LYP hybrid exchange correlation functional and the 6-31^{++}G** basis set [30–32]. An energy minimized structure was exported to Gaussian03 and reminimized with 6-31^{++}G** followed by calculation of spectroscopic properties [33]. The theoretical absorption frequencies were scaled by 0.98 to allow a more facile comparison to experiment. The theoretical spectra were obtained from the calculated frequencies, dipole and rotational strengths using a Lorentzian fitting with a half width of 4 cm^{-1}. For all three compounds calculations were performed on the enantiomers having the (*R*)-configuration at the benzylic position.

Transition state modeling was performed using the MMFFs force field [34] as incorporated in MacroModel v8.0 [35]. The structures were obtained by restraining the lengths of the two forming C–O bonds to 2.30 Å (C_α–O) and 2.00 Å (for O–C_β), in both cases using a force constant of 1,000 kJ/(mol Å^2). The breaking O–O bond was restrained to 1.85 Å using a similar force constant. The O–O–C_α and O–O–C_β angles were both restrained to 160° using a force constant of 100 kJ mol^{-1} rad^{-2}. Finally, the C–O–C_α–C_β dihedral was restrained to either 90° (*spiro*-TS) or 180° (*planar*-TS) using the standard force constant of 100 kJ mol^{-1}.

All VA and VCD experiments were carried out on a Thermo-Nicolet Nexus 870 FTIR instrument equipped with a VCD compartment. Properties used to convert the experimentally determined absorbances to molar extinction coefficients: Mw: 148.2 g mol^{-1}, the density for (*1R*)-2, 2-dimethylphenyloxirane (**3**) was found in the literature to be 0.93 g cm^{-3} at 20°C [36]. This value was also used for the two other compounds in this study.

Experiments on neat samples were carried out using a cell with BaF_2 windows and a 25 μm spacer. Experiments on 1.3 M samples of **1–3** in CCl_4 were carried out in a sealed KBr cell with a path length of 100 μm. In all cases the VCD spectrum was determined using an optically active sample and the corresponding racemic sample as background, running 30,000 scans with a resolution of 4 cm^{-1} (collection time: 8 h). The photoelastic modulator was set at 1,500 cm^{-1}. The three alkene substrates were synthesized as pure stereo- and regioisomers using a literature procedure [37]. The racemic epoxides were synthesized as reported previously using *m*-chloroperoxybenzoic acid (*m*CPBA) in dichloromethane [38]. The optically active epoxides were synthesized using the general procedure described below [14]:

The alkene (20 mmol, 2.64 g) was dissolved in a 1:2 mixture of acetonitrile and dimethoxymethane (300 mL). Bu_4NHSO_4 (0.80 mmol, 300 mg) was added, followed by 1, 2:4, 5-di-*O*-isopropylidene-D-erythro-2, 3-hexodiuro-2, 6-pyranose (6 mmol, 1.55 g). A solution of Oxone (17 g, 32 mmol) in aqueous Na_2(EDTA) (4×10^{-4} M, 130 mL) and a solution of K_2CO_3 (16 g, 116 mmol) in water (130 mL) were added dropwise separately over a period of 1 h (via addition funnels). After 2 h the reaction mixture was transferred to a separatory funnel with water (300 mL) and pentane (300 mL). The organic phase was extracted twice with pentane (300 mL), washed with brine (300 mL) and then dried over $MgSO_4$. After removal of the solvents, silica gel chromatography was performed using 5% ether in pentane as eluent to give the desired epoxides **1–3** in good yields (see subsequently).

In all cases enantiomeric excess was determined by GC on a Shimadzu GC-2010 equipped with a Chrompack CP Chirasil-Dex CB 0.25 mm × 25 m column (isothermal 90°C). The racemic reference material had identical ^{1}H and ^{13}C spectra and yielded two fully separated peaks of equal area on chiral GC. GC-HRMS was performed on a Waters Micromass GCT equipped with an Agilent DB-5MS column.

(*1R, 2R*)-1,2-dimethylphenyloxirane (**1**) was isolated as a clear oil in 80% yield (2.36 g). GC retention times were 17.08 and 17.26 min, respectively, for the two enantiomers and the enantiomeric excess was determined to be 97%.

^{1}H NMR (300 MHz, $CDCl_3$, δ): 1.43 (d, 5.4 Hz, 3H), 1.67 (s, 3H), 2.95 (q, 5.4 Hz, 1H), 7.22–7.38 (m, 5H) [14].

^{13}C NMR (75.4 MHz, CDCl3, δ): 14.7, 17.6, 60.6, 62.8, 125.3, 127.4, 128.5, 143.3.

Exact mass calculated for $C_{10}H_{12}O$: 148.0888, found 148.0887.

(*1R,2S*)-1,2-dimethylphenyloxirane (**2**) was isolated as a clear oil in 81% yield (2.44 g). GC retention times were 12.8 and 13.8 min, respectively, for the two enantiomers and enantiomeric excess was determined to be 80%.

^{1}H NMR (300 MHz, CDCl3, δ): 0.98 (d, 5.4 Hz, 3H), 1.64 (br s, 3H), 3.17 (q, 5.4 Hz, 1H), 7.23–7.38 (m, 5H) [39].

^{13}C NMR (75.4 MHz, CDCl3, δ): 14.7, 24.8, 61.5, 62.9, 126.8, 127.3, 128.3, 139.9.

Exact mass calculated for $C_{10}H_{12}O$: 148.0888, found 148.0887.

(*1R*)-2,2–Dimethylphenyloxirane (**3**) was isolated as a clear oil in 82% yield (2.43 g). GC retention times were 15.29 and 15.68 min, respectively, for the two enantiomers and enantiomeric excess was determined to be 66%.

^{1}H NMR (300 MHz, CDCl3, δ): 1.08 (s, 3H), 1.49 (s, 3H), 3.87 (s, 1H), 7.24–7.39 (m, 5H) [40].

^{13}C NMR (75.4 MHz, CDCl3, δ): 18.2, 25.0, 61.3, 64.8, 126.6, 127.6, 128.3, 136.8 [40].

Exact mass calculated for $C_{10}H_{12}O$: 148.0888, found 148.0900.

Supporting Information Available: XYZ coordinates and SCF energies for all structures discussed in the text and calculated spectral properties (vibrational frequencies, dipole strengths and rotational strengths) are available as supporting information.

Acknowledgments The Center for Sustainable and Green Chemistry and the Quantum Protein Centre are sponsored by the Danish National Research Foundation. KJJ would like to acknowledge the Western Australian government for the Premier Fellowship Program for financial support and J.D. Gale for interesting and thoughtful discussions.

References

1. Jacobsen EN (2000) Acc Chem Res 33:421
2. Taylor SK (2000) Tetrahedron 56:1149
3. Hanson RM (1991) Chem Rev 91:437
4. Pfenninger A (1986) Synthesis 89
5. Behrens CH, Sharpless KB (1983) Aldrichimica Acta 16:67
6. Besse P, Veschambre H (1994) Tetrahedron 50:8885
7. Katsuki T, Sharpless KB (1980) J Am Chem Soc 102:5974
8. Johnson RA, Sharpless KB (2000) In: Ojima I (ed) Catalytic asymmetric synthesis, Chap. 6A, 2nd edn. Wiley-VCH, New York
9. Zhang W, Loebach JL, Wilson SR, Jacobsen EN (1990) J Am Chem Soc 112:2801
10. Jacobsen EN, Wu MH (1999) In: Jacobsen EN, Pfaltz A, Yamamoto H (eds) Comprehensive asymmetric catalysis, Chap. 18.2. Springer, Berlin Heidelberg New York

11. Irie R, Noda K, Ito Y, Matsumoto N, Katsuki T (1990) Tetrahedron Lett 31:7345
12. Katsuki T (2000) In: Ojima I (ed) Catalytic asymmetric synthesis, Chap. 6B, 2nd edn. Wiley-VCH, New York
13. Shi Y (2004) Acc Chem Res 37:488
14. Wang Z-X, Tu Y, Frohn M, Zhang J-R, Shi Y (1997) J Am Chem Soc 119:11224
15. Wang Z-X, Tu Y, Frohn M, Shi Y (1997) J Org Chem 62:2328
16. Tu Y, Wang Z-X, Shi Y (1996) J Am Chem Soc 118:9806
17. Wang Z-X, Miller SM, Anderson OP, Shi Y (1999) J Org Chem 64:6433
18. Tu Y, Wang Z-X, Frohn M, He M, Yu H, Tang Y, Shi Y (1998) J Org Chem 63:8475
19. Shu L, Wang P, Gan Y, Shi Y (2003) Org Lett 5:293
20. Tian H, She X, Shi Y (2001) Org Lett 3:715
21. Tian H, She X, Shu L, Yu H, Shi Y (2000) J Am Chem Soc 122:11551
22. Tian H, She X, Xu J, Shi Y (2001) Org Lett 3:1929
23. Singleton DA, Wang Z (2005) J Am Chem Soc 127:6679
24. Fristrup P, Lassen PR, Johannesen C, Tanner D, Norrby P-O, Jalkanen KJ, Hemmingsen L (2006) J Phys Chem A 110:9123
25. The visualizations have been performed using Jmol, An OpenScience Project, © 2004 by the Jmol Team, see also http://www.jmol.sourceforge.net
26. Jalkanen KJ, Würtz Jürgensen V, Degtyarenko IM (2005) Adv Quant Chem 50:91
27. Ashvar CS, Devlin FJ, Stephens PJ (1999) J Am Chem Soc 121:2836
28. Molecular modelling was carried out in MacroModel v. 8.0 from Schrodinger Inc., http://www. schrodinger.com.
29. Jaguar 4.2, Schrödinger, Inc., 1500 SW First Avenue, Suite 1180, Portland, OR 97201. For the most recent version, see: Schrodinger Inc. (http://www.schrodinger.com)
30. Clark T, Chandrasekhar J, Spitznagel GW, Schleyer PvR (1983) J Comp Chem 4:294
31. Hehre WJ, Ditchfield R, Pople JA (1972) J Chem Phys 56:2257
32. Ditchfield R, Hehre WJ, Pople JA (1971) J Chem Phys 54:724
33. Gaussian 03, Revision C.02, Frisch MJ, Trucks GW, Schlegel HB, Scuseria GE, Robb MA, Cheeseman JR, Montgomery JA Jr, Vreven T, Kudin KN, Burant JC, Millam JM, Iyengar SS, Tomasi J, Barone V, Mennucci B, Cossi M, Scalmani G, Rega N, Petersson GA, Nakatsuji H, Hada M, Ehara M, Toyota K, Fukuda R, Hasegawa J, Ishida M, Nakajima T, Honda Y, Kitao O, Nakai H, Klene M, Li X, Knox JE, Hratchian HP, Cross JB, Bakken V, Adamo C, Jaramillo J, Gomperts R, Stratmann RE, Yazyev O, Austin AJ, Cammi R, Pomelli C, Ochterski JW, Ayala PY, Morokuma K, Voth GA, Salvador P, Dannenberg JJ, Zakrzewski VG, Dapprich S, Daniels AD, Strain MC, Farkas O, Malick DK, Rabuck AD, Raghavachari K, Foresman JB, Ortiz JV, Cui Q, Baboul AG, Clifford S, Cioslowski J, Stefanov BB, Liu G, Liashenko A, Piskorz P, Komaromi I, Martin RL, Fox DJ, Keith T, Al-Laham MA, Peng CY, Nanayakkara A, Challacombe M, Gill PMW, Johnson B, Chen W, Wong MW, Gonzalez C, Pople JA (2004) Gaussian, Inc., Wallingford
34. Halgren TA (1996) J Comput Chem 17:490
35. MacroModel v. 8.0 from Schrodinger Inc.: Mohamadi F, Richards NGJ, Guida WC, Liskamp R, Lipton M, Caulfield C, Chang G, Hendrickson T, Still WC (1990) J Comput Chem 11:440. For current versions, see: http://www.schrodinger.com
36. Razuvaev GA et al. (1965) J Org Chem USSR (Engl Transl) 1:1589–1591
37. Fristrup P, Tanner D, Norrby P-O (2003) Chirality 15:360
38. Fristrup P, Dideriksen BD, Tanner D, Norrby P-O (2005) J Am Chem Soc 127:13672
39. Satoh T, Kobayashi S, Nakanishi S, Horiguchi K, Irisa S (1999) Tetrahedron 55:2515
40. Pedragosa-Moreau S, Archelas A, Furstoss R (1996) Tetrahedron 52:4593